Aerodynamic and geometric optimization for the design of centrifugal compressors

A. Perdichizzi and M. Savini*

Maximizing efficiency is the main goal in centrifugal compressor design. Thus a computer code has been developed to optimize geometric and fluid dynamic variables with respect to several design constraints. Computations are performed with an adiabatic one-dimensional approach using state-of-the-art loss and slip correlations. The optimization takes into account mechanical stress limits. Results with different loss and slip correlations are compared with the available experimental data. Changes in optimum efficiency and specific speed due to variations of mass flow rate and pressure ratio are also presented and discussed together with the trends of the optimum geometric features.

Keywords: *compressors, fluid dynamics, design*

Centrifugal compressors are widely used in small aeronautic and industrial gas turbines and in turbochargers for internal combustion engines. The main demand is to achieve the highest possible efficiency, especially for highly loaded machines, ie at high compression ratios. Numerous theoretical and experimental investigations are aimed at resolving the fluid dynamic problems and improving the design criteria.

The great number of geometric and fluid dynamic variables and their interactions make it hard to choose the best values for any given project using simple design criteria. To overcome this obstacle, the authors have developed a computer code which uses a mathematical optimization algorithm for maximizing efficiency.

Flow model

Since the results of the optimization process are strictly dependent on the flow model accuracy, it is necessary to take into account, even if in an approximate way, the complex fluid dynamic phenomena, including boundary layer growth, jet-wake formation, shock waves and boundary layer interaction, etc, in a centrifugal compressor. One must also choose carefully the loss model, because the available methods, by their very nature always have an element of empiricism. Indeed, they are based on a limited number of machines and problems may arise when they are applied to others. To overcome this drawback the authors tested several methods[1-5] to find the most comprehensive for the medium-to-high compression ratios.

Thermodynamic and fluid dynamic quantities are computed in the one-dimensional approach at five stations according to the following scheme (Fig 1):

1 – rotor inlet
2 – rotor discharge
3 – vaned diffuser leading edge
4 – vaned diffuser throat
5 – vaned diffuser outlet

* Dipartimento di Energetica, Politecnico di Milano, Piazza Leonardo da Vinci 32, Milano, Italy
Received 14 May 1984 and accepted for publication on 22 August 1984

Rotor

Hub, mid-flow and tip quantities at the rotor inlet are computed both outside and inside the blade row; trailing edge thicknesses are considered and an optimum incidence, ie minimum losses, is assumed. Station 2 is solved evaluating dissipation in the flow field across the entire impeller. Fluid dynamic losses may be estimated in two alternative ways:

Northern Research method[2]

With the one dimensional limitation, this method carries out a detailed analysis of the flow within the impeller. Albeit roughly, the relative velocity distributions on the suction and pressure sides of the blade are considered. On the basis of these distributions, the various losses are evaluated and the jet-wake development estimated assuming that separation occurs if $W/W_{max} < 0.56$ and that, beyond the separation point, diffusion ceases and W is a constant. Thus the wake extension and the jet quantities at the impeller exit can be determined.

Dissipative phenomena considered in evaluating losses are:

Inducer incidence at the design point;
Skin friction along the blade channel;
Blade loading;
Mixing between jet and wake according to the Johnston and Dean model[6];
Tip blade leakage;
Disc friction.

The method is also applicable to impellers with splitter blade rows.

Galvas' method[3]

This method is less detailed than the one above, not allowing for the relative velocity distribution. In spite of its simplicity, it takes into account the main loss factors and gives reasonable results. Losses considered are:

Incidence;
Skin friction;
Blade loading;

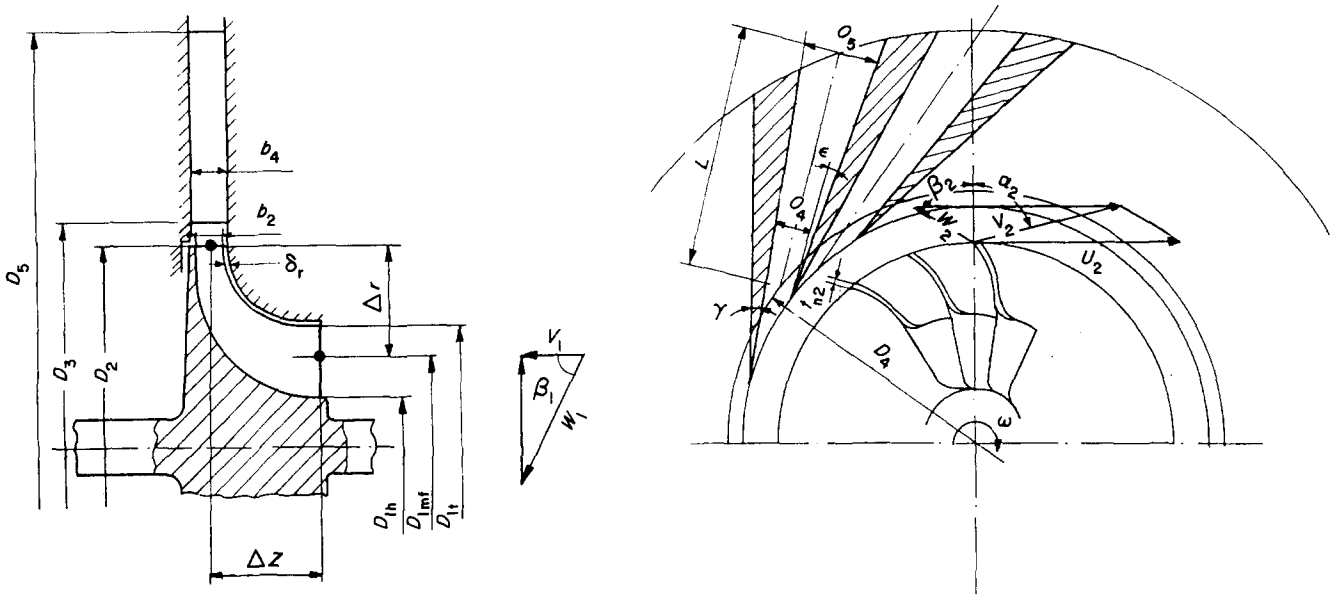

Fig 1 Geometric configuration of the compressor

Notation

a	Speed of sound
A	Geometric area
b	Axial depth
C_p	Pressure recovery coefficient
D	Diameter
L	Diffuser length
L_{eu}	Eulerian work
K_b	Blockage factor
$\dot{m}$	Mass flow rate
M_v	Absolute Mach number
M_w	Relative Mach number
n	Rotational speed, r/s
N_s	Specific speed, $n \cdot \dot{V}_{in}^{1/2}/\Delta h_{is}^{3/4}$
o	Diffuser throat width
p	Pressure
r^*	Isentropic degree of reaction
U	Tangential velocity
V	Absolute velocity
W	Relative velocity
t_n	Normal blade thickness
T	Temperature
$\dot{V}$	Volume flow rate
X_{sp}	% meridional length at splitter
Z	Number of blades
α	Absolute velocity angle
β	Relative velocity angle
β'	Geometric blade angle
δ	Clearance between impeller and shroud
Δh_{ext}	External losses
Δh_{is}	Isentropic head
Δ_r	Impeller radial extent
φ	Flow coefficient, V_r/U_2
π	Pressure ratio
ε	Diffuser half-divergence angle
μ	Slip factor
ψ	$(V_{tg}/U)_2$
σ	Mechanical stress

Subscripts

ax	Axial
D	Diffuser
h	Hub
I	Impeller
mf	Mean flow
OV	Overall
r	Radial
ref	Reference conditions
t	Tip
tg	Tangential
VL	Vaneless diffuser
VD	Vaned diffuser
TS	Total/static
TT	Total/total
0	Stagnation conditions
1	Rotor inlet
2	Rotor outlet
3	Vaned diffuser inlet
4	Diffuser throat
5	Diffuser exit
$\Delta\eta_{BL}$	Blade loading losses
$\Delta\eta_{CL}$	Clearance losses
$\Delta\eta_{DF}$	Disc friction losses
$\Delta\eta_{INC}$	Incidence losses
$\Delta\eta_{MIX}$	Mixing losses
$\Delta\eta_{SF}$	Skin friction losses
$\Delta\eta_{VL}$	Vaneless diffuser losses
$\Delta\eta_{VD}$	Vaned diffuser losses
$\Delta\eta_{EX}$	Kinetic energy discharge losses

Units are SI, angles are measured from the meridional direction

Disc friction;
Backflow.

The mixing loss is included in the global loss while the backflow loss also includes the clearance leakage loss.

The slip correlations commonly quoted in the literature and used here to compute the exit flow angle α_2 are the Wiesner formulation[7]:

$$\mu = 1 - \frac{(\cos \beta'_2)^{0.5}}{Z_I^{0.7}}$$

and the Eckert formulation[8] as modified by the Northern Research to consider the relative velocity deceleration ratio:

$$\mu = \frac{1}{1 + (1 + K_1 (W_{1t}/W_2)^2)(K_2 \cos \beta'_2) \Big/ \left(Z_I \left(1 - \frac{D_{1s} + D_{1t}}{2D_2} \right) \right)}$$

Vaneless diffuser

The equations of motion are solved at an appropriate number of stations using the classical Stanitz approach with regard to friction and heat exchange[9]. The aerodynamic blockage due to the growth of the boundary layer along the sidewalls and the joint losses are taken into account.

Vaned diffuser

The entrance region is extremely important since the flow is unsteady, often transonic, and the viscous effects are significant: special attention has therefore been paid to its modelling. The diffuser performance and the pressure recovery coefficient C_p are strongly related to the boundary layer growth up to the throat since a boundary layer that is well developed and near to separation may prevent the diffusion process. Since it is impossible to predict accurately the boundary layer in that region, a simplified method proposed by Dean[1] allows one to estimate the throat blockage once the pressure rise from the rotor discharge is known. When the flow is supersonic at the diffuser leading edge, it is assumed to become subsonic by means of a normal shock wave: this makes it possible in the one-dimensional representation to take into account the shock wave-boundary layer interaction, in as much as the shock pressure rise leads to a higher blockage. This is substantially confirmed by Kenny's results[10].

It is assumed that only straight channel diffusers are used as this work refers mainly to high pressure ratio machines. The design criteria and the performance evaluation are derived from Dean and Runstadler's Diffuser Data Book[11], assuming as independent variables the throat Mach number M_{t_4}, the blockage factor K_{b_4} and the aspect ratio b_4/O_4.

Each set of these parameters is joined to the optimum geometry $(A_5/A_4, \varepsilon)$ suggested by the maps given by Dean and Runstadler. The optimum is determined by the highest $C_{p_{vd}}$ and the smallest area ratio able to warrant stable operating conditions, that is far enough away from the region of unsteady stall. In this way a certain range for the off-design performance is ensured. The positive influence of the inlet swirl, compared with the uniform test conditions, is treated in the manner suggested by Stevens and Williams[12]. Once the diffuser geometry is defined, it is possible to evaluate the diffuser performance by means of two other methods:

Northern Research method:

This divides the diffuser into two zones, before and after the throat. The losses in the first part depend substantially on the Mach number and rise, causing the latter to approach unity; the other losses are due to throat Mach number, blockage and area ratio.

Galvas' method:

This uses Dean and Runstandler's data in a simplified mode, for instance without accounting for the aspect ratio and for the divergence angle ε.

Optimization strategy

Solving the optimization problem requires:

Design specifications, namely mass flow rate, pressure ratio, thermodynamic properties of the working fluid and inlet conditions.

Project variables; eleven independent variables (Table 1) allow one to fix the machine geometry and to compute the efficiency. Blade thicknesses and the clearance gap are determined as functions of the rotor outlet diameter, with respect to technological limits.

Target function; the function to be optimized is the overall compressor efficiency. In some cases it may be useful to optimize the total-to-static efficiency; in others the static-to-static efficiency is optimised. The kinetic energy recovery factor Φ_E is introduced therefore to cover both definitions:

$$\eta = \frac{\Delta h_{is} + \Phi_E V_5^2/2}{L_{eu} + \Delta h_{ext}}$$

where L_{eu} is the Eulerian work and Δh_{ext} is the 'external' losses.

Constraints; several geometric and fluid dynamic constraints limit the search field. These constraints must be observed if physically meaningful and/or practically feasible solution are to be found. In addition, mechanical stress limitations within the rotor must be considered; the critical regions are: the blade root at the outer diameter owing to the bending stress; the blade root at about half the radial extent owing to the sum of the bending and centrifugal tensile stresses; and the bore because of centrifugal force.

The stresses at these points are evaluated on the basis of Osborne's simplified criteria[13] and are compared

Table 1 Variables and design specifications

Optimization variables
D_{1t}, D_{1h}, D_2, β'_2, b_2, Z_I, Δ_z/Δ_r, D_3/D_2, b_3/b_2, Z_D, x_{sp}

Depent variables
δ = max (0.3 mm, or $D_2/400$)
t_{n1min} = max (0.2 mm, or $D_2/500$)
t_{n2min} = max (0.6 mm, or $D_2/200$)
$t_{nt}/t_{nh} = 0.33$

Design data
- Fluid thermodynamic properties
- Inlet conditions
- Pressure ratio
- Maww flow rate
- Wheel alloy

with the yield stress which depends upon the temperature level and the alloy used. All these constraints are shown in Table 2.

Mathematical optimization; the numerical procedure used is able to optimize a function with up to 30 variables and 90 constraints (40 linear in the independent variables and 50 non-linear).

The search requires numerous attempts (about 4000) with different sets of variables; each one performs a full design and performance evaluation of the compressor. The time taken to solve a sample case is about 300 seconds of CPU on a UNIVAC 1100/80 computer.

Results

The reliability of the loss correlations was checked for various compressors by comparing predicted performances for the actual geometries with the experimental data. Table 3 is an example of these comparisons for two machines, one built by Franco Tosi SpA and the other by Nuovo Pignone SpA, for which detailed measurements were available.

The Northern Research method, coupled with the Dean and Runstadler method for the diffuser, gives the most accurate results. The overall efficiency, the loss distributions and the specific speed are close to those of the real machines, and is confirmed by the results of the optimizations, an example of which is presented in Table 4. Nevertheless, the geometry turns out to be dissimilar because the optimum solution involves larger blade heights which generate lower deceleration ratios W_2/W_{1t} and flow coefficients ϕ. In the actual compressor a smaller ratio b_2/D_2 is adopted to get a lower $\lambda = V_t/V_r$, thus ensuring a wider off-design range at low flow rates.

The optimization results show that, even if the optimum efficiency and specific speed are nearly the same, the fluid dynamic and geometric configuration tends to correspond to the loss model trying to cut down the most critical losses:

the Galvas method leads to too low efficiencies, as in Table 3, because the rotor is over-penalized. Thus the best solution is characterized by lower N_s and r^* and by a more radial β'_2;

the full Northern Research method over-estimates the vaned diffuser losses and the optimization tends to overload the impeller adopting larger D_2 and β'_2.

Table 5 shows the influence of the slip correlation on the optimization.

It is important to note that although Wiesner's correlation gives a higher slip factor, the solution is similar in terms of efficiency and fluid dynamic quantities. The difference in the blade angle makes up for the slip formulation so as to obtain an identical flow angle. Hence one can say that the results are not seriously affected by the type of correlation used. It seemed more advisable to employ Eckert's correlation because it takes into account the deceleration ratio W_2/W_{1t} and this may become important at high pressure ratios.

To test the importance of the impeller material, a comparison was made between two optimizations for the same design conditions ($\pi = 5$, $\dot{m} = 2.45$ Kg/s). In the first case an aluminium alloy was used while titanium was used in the second (Table 6). The first case gave lower efficiency because blade backward leaning is limited (17° versus 40°)

Table 2 Constraints on optimization

1. *Geometric*	2. *Fluid dynamics*	
$20° < \beta'_{1t} < 70°$	$M_{w1t} < 1.4$	$0 < C_{pvl} < 0.4$
$0.4 < D_{1t}/D_2 < 0.7$	$M_{w1m} < 0.9$	$\varepsilon_{wake} < 0.8$
$0.3 < D_{1h}/D_{1t} < 0.7$	$W_{min1} > 0$	$K_{bax} < 0.5$
$0.03\,m < D_2 < 2\,m$	$W_2/W_{1t} > 0.25$	
$0° < \beta_2 < 60°$	$\lambda < 4$ $(\alpha_2 < 76°)$	
$0.01 < b_2/D_2 < 0.4$		
$8 < Z_I < 60$		
$0.8 < D_2/D_r < 1.2$	3. *Mechanical stress*	
$0.4 < X_{SP} < 0.6$	$\sigma_A < \sigma_{limA}$	
$1.05 < D_3/D_2 < 1.2$	$\sigma_B < \sigma_{limB}$	
$0.8 < b_3/b_2 < 1.2$	$\sigma_C < \sigma_{limC}$	
$0.2 < b_4/O_4 < 7.0$		
$10 < Z_D < 80$		
$4\,mm < O_4$		
$5° < \gamma < 30°$ (Fig. 1)		
$D_5/D_2 < 2.0$		

Table 3 Comparison of results

	η_{TS}	$\Delta\eta_I$	$\Delta\eta_{VL}$	$\Delta\eta_{VD}$	N_S	ψ	ϕ
Galvas	79.4	6.3	2.25	6.4	0.124	0.712	0.30
NR*	76.3	6.3	2.4	9.5	0.128	0.72	0.27
NR+DR†	82.3	6.3	2.22	6.0	0.122	0.71	0.31
Real	84.0	4.8	1.71	6.1	0.121	0.71	0.42
F. TSOI compressor	$\pi = 2.4$	$\dot{m} = 1.95$ Kg/s	$N = 28\,000$ r/min				
	$\beta'_2 = 25°$	$D_2 = 0.257$ m	$Z_I = 16$				
	$\varepsilon = 4°$	$b_4/O_4 = 0.99$	$Z_D = 25$				
Galvas	80.4	6.17	1.84	5.8	0.124	0.673	0.194
NR*	78.6	5.8	2.13	7.6	0.126	0.674	0.193
NR+DR†	82.0	5.8	1.8	6.0	0.123	0.67	0.20
Real	82.5	–	–	–	0.123	0.67	0.20
N. Pignone compressor	$\pi = 2.45$	$\dot{m} = 4.3$ Kg/s	$N = 20\,000$ r/min				
	$\beta'_2 = 50°$	$D_2 = 0.385$ m	$Z_I = 16$				
	$\varepsilon = 4°$	$b_4/O_4 = 0.716$	$Z_D = 15$				

** Northern Research method*
† Northern Research coupled with Dean and Runstadler's method for the diffusor

Table 4 Optimization results $\pi=2.4$, $\dot{m}=1.95$ kg/s

	η_{TS}	$\Delta\eta_I$	$\Delta\eta_{VL}$	$\Delta\eta_{VD}$	N_s	ψ	ϕ	r^*	β'_2	b_2/D_2
Galvas	80.6	5.8	1.1	5.2	0.111	0.76	0.22	0.64	26	0.057
NR	81.8	5.4	0.8	5.8	0.122	0.56	0.20	0.76	55	0.047
NR+DR	83.3	4.8	0.87	5.1	0.117	0.73	0.20	0.67	34	0.071
Real	84.0	4.8	1.71	6.1	0.121	0.71	0.42	0.58	25	0.044

Table 5 Effect of slip correlation on optimization

Slip correlation	μ	η_{TS}	N_s	ϕ	ψ	W_2/W_{1t}	β_2	β'_2
Wiesner	0.867	0.834	0.120	0.22	0.71	0.58	53.4	40
Eckert	0.842	0.833	0.118	0.20	0.73	0.53	53.5	34

Table 6 Impeller material comparison $\pi=5$, $\dot{m}=2.45$ kg/s

Impeller alloy	η_{TS}	N_s	ϕ	ψ	r^*	B'_2	U_2	W_2/W_{1t}	M_{w1t}	$Mv2$
Aluminium	0.801	0.097	0.22	0.86	0.61	17	502	0.41	0.92	1.1
Titanium	0.827	0.109	0.20	0.73	0.67	40	535	0.53	0.99	0.99

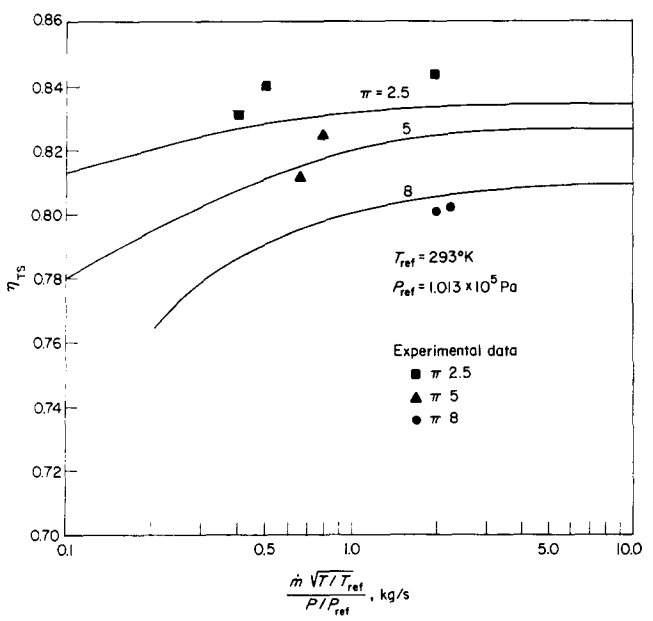

Fig 2 Total-to-static efficiency versus mass flow rate and pressure ratio

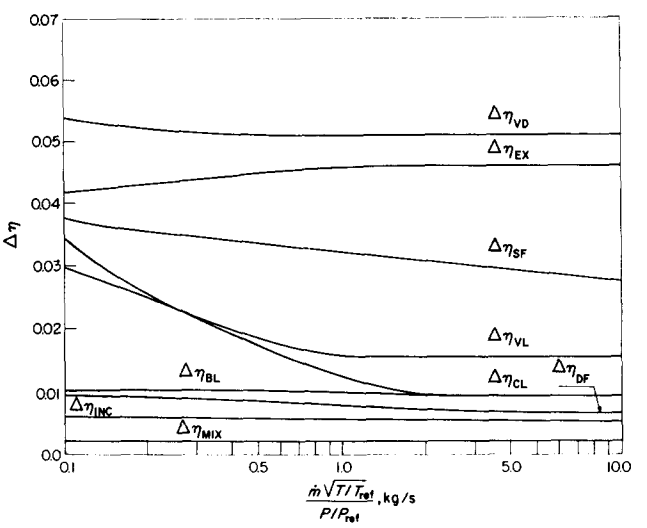

Fig 3 Losses at different flow rates ($\pi=5$)

to avoid exceeding the yield stress at the blade root. Thus the rotational speed and the degree of reaction are lower, decreasing the efficiency.

Flow rate and pressure ratio variation

These results refer to air compressors and assume a titanium alloy to be used since it allows better performance.

Fig 2 shows efficiency versus mass flow rate and pressure ratio. Note that the performance of actual compressors[22] are in good agreement with the results, supporting the flow model and loss formulation accuracy.

The decreased efficiency at lower flow rates is due to the size reduction; in fact as one can see in Fig 3, which shows the trend of the losses, the effect of the leakage rises sharply since the tip gap has a lower limit of $\delta_{min}=0.2$ mm, which is fixed by technological considerations. The frictional losses through the machine also rise because of lower Reynolds numbers and higher relative roughness. This is not noticeable in the vaned diffuser since the trend is counterbalanced by a lower aerodynamic loading. In fact, at lower flow rates the geometric limitations on O_{4min} and $(D_5/D_2)_{max}$ tend to transfer part of the loading from the vaned diffuser to the vaneless diffuser by increasing D_3/D_2.

The optimum specific speed (Fig 4) at equal pressure ratio is almost constant, with respect of the similarity rules, over a wide range of mass flow rates.

The curves of the geometric ratios D_{1t}/D_2 and

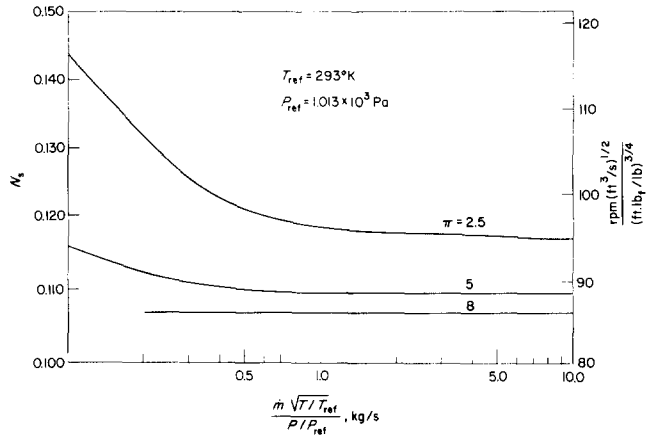

Fig 4 Optimum specific speed at different flow rates and pressure ratios

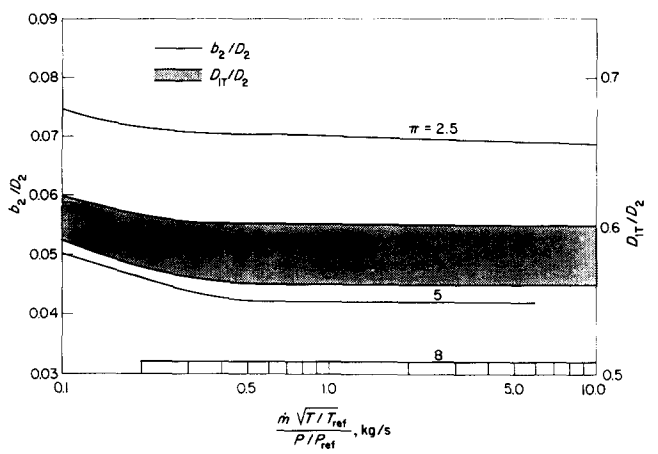

Fig 5 Non-dimensional geometric features of the impeller (D_{1t}/D_2, b_2/D_2)

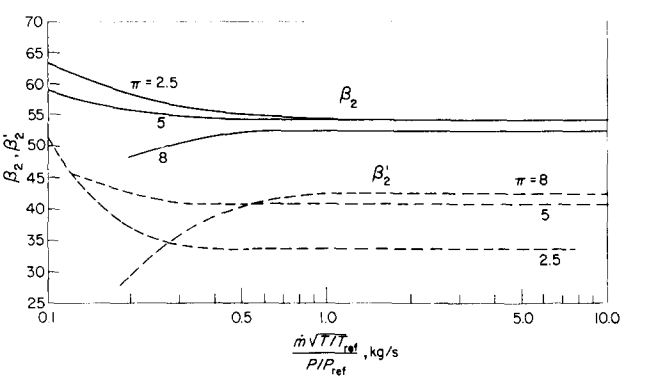

Fig 6 Kinematic (β_2) and geometric (β_2') angles at the rotor discharge

b_2/D_2 substantially confirm the above statement (Fig 5).

At small flow rates N_s tends to rise because the number of blades decreases with the size (Fig 8) and the blade loading loss increases: thus the optimum solution moves toward higher β_2 (Fig 6) and r^* (Fig 7) with an appreciable increase in the rotational speed.

The specific speed changes inversely with the pressure ratio for stress reasons; in fact there are two ways to limit the blade root bending stress: decrease blade height b_2, increasing D_2 and reducing the rotating speed; or making the blade exit angle more radial (smaller β_2') to reduce the tangential velocity. The former solution is more advisable as the increase in clearance losses is less than the blade loading and mixing losses due to the greater extension of the wake in the latter case.

Fig 6 shows geometric and kinematic angles at the rotor discharge: note that the optimum flow angle remains nearly constant, at 50°–55°, although the blade angle varies with the pressure ratio. It follows that the slip factor increases with π: in fact highly loaded machines need a greater number of blades in order to reduce the aerodynamic loading.

Fig 7 shows that the pressure ratio does not influence the degree of reaction r^* and the deceleration ratio W_2/W_{1t}, except at small flow rates. For mass flow rates greater than 0.5 Kg/s the optimum degree of reaction is always 0.67 and the deceleration ratio is slightly lower than the value referred to as threshold of separation, $W_2/W_{1t} = 0.56$.

Mach numbers graphs (Fig 9) show that at low π M_{V_2} is greater than M_{w1t}, but, at high pressure ratio, this trend is reversed. In fact keeping low M_{V_2} helps reduce the rise of the throat blockage K_{b_4}, a major factor in diffuser performances. From Fig 10 it is possible to assess the optimum shape of the vaned diffuser. As the pressure ratio

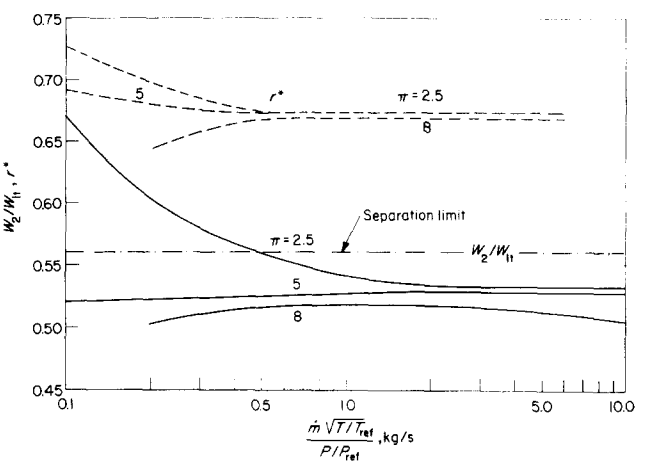

Fig 7 Isentropic degree of reaction and rotor deceleration ratio (W_2/W_{1t})

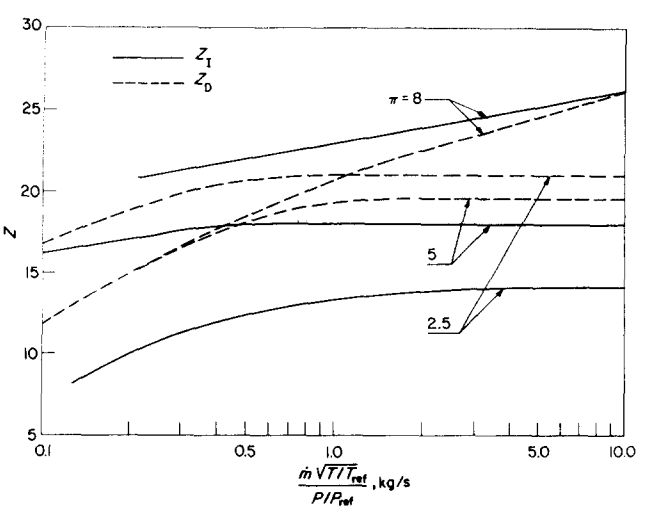

Fig 8 Optimum numbers of impeller blades and diffuser vanes

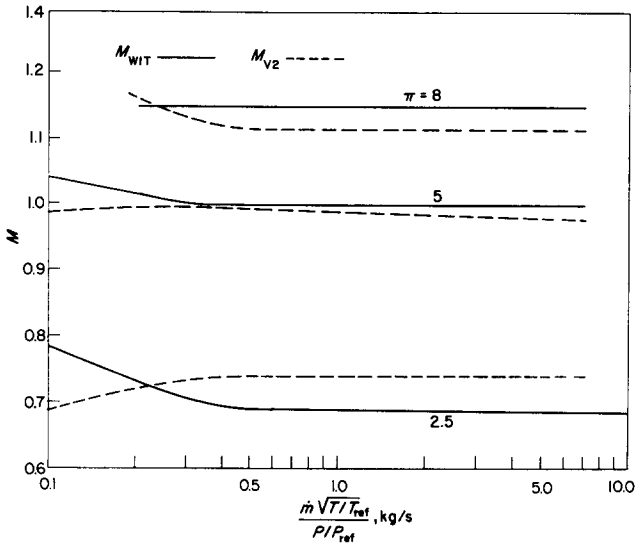

Fig 9 Mach numbers (M_{w1t}, M_{v2})

goes up, the worsening throat conditions (K_{b_4} and M_{V4}) reduce the pressure recovery $C_{p_{vd}}$ and the area ratio A_5/A_4 that the diffuser can sustain. The decrease in the aspect ratio b_4/O_4 for small flow rates implies a greater divergence angle.

Closing remarks

The analysis of the results compared with 'state-of-the-art' performance and with the experimental data of actual centrifugal compressors confirms that the optimization method presented in this paper is able to provide trustworthy predictions.

The investigation at different flow rates and pressure ratios showed how small machines suffer the major penalty of dimensional effects, for example clearances, thicknesses, Reynolds numbers, and how consequently the optimum specific speed becomes greater. At the higher pressure ratios the overall efficiency decreases more sharply since N_s cannot increase because of mechanical stress limitations. The diagrams presented may be helpful in the design of centrifugal compressors since they supply the best N_s and geometric features to obtain the highest possible level of efficiency.

Acknowledgements

The authors wish to thank Franco Tosi SpA for placing loss correlations and experimental measurements at their disposal, and Nuovo Pignone SpA for providing data of their compressor.

References

1 **Dean R. C.** The fluid dynamic design of advanced centrifugal compressors. *TN 153, 1972, Creare Inc., Hanover, USA*

2 An engineering research program for centrifugal compressors: revised prediction procedures. *Northern Research N. 1143–38, Dec 1971*

3 **Galvas M.R.** Fortran program for predicting off-design performance of centrifugal compressors. *NASA TN 07487, Nov 1973*

4 **Baljé O.E.** Loss and flow path studies on centrifugal compressors. *ASME paper 70-GT-12, 1970*

5 **Mashimo T., Watanabe I. and Ariga I.** Effect of Reynolds numbers on performance characteristics of a centrifugal compressor, with special reference to configurations of impellers. *J. Eng. for Power, July 1975*

6 **Johnston J.P. and Dean R.C.** Losses in vaneless diffusers of centrifugal compressors and pumps. *J. Eng. for Power*, **88**, *(1) 1966*

7 **Weisner F.J.** A review of slip factors of centrifugal impellers. *J. Eng. for Power*, **89**, *1967*

8 **Eckert, B. and Schnell E.** Axial und radial kompressoren, *Springer Verlag Berlin, 1961*

9 **Stanitz J.D.** One-dimensional compressible flow in vaneless diffusers of radial and mixed-flow centrifugal compressors, including effects of friction, heat transfer and area change. *NACA TN 2610, 1952*

10 **Kenny D. P.** Supersonic radial diffusers. *AGARD Lecture notes 39, Advanced compressors, Von Karman Institute, Brussels, 1–4 June 1970*

11 **Runstadler P., Dolan F. and Dean R.** Diffuser data book. *TN 186 Creare Inc., May 1975*

12 **Stevens S. J. and Williams G. J.** The influence of inlet conditions on the performance of annular diffusers. *J. Fluid Eng.* **102**, *Sept 1980*

13 **Osborne C.** Preliminary structural considerations in centrifugal compressors. *Lecture notes on Advanced Concepts in Centrifugal Compressors Design and Performance, Paris, 16–20 May 1983*

14 **Buzzi Ferraris M.** *Subroutine OPTNOV. CILEA TN, Milan, 1976*

15 **Chevis R. W. and Varley R. J.** Centrifugal compressors for small aero- and automotive gas turbine engines. *AGARD CP 282 Centrifugal Compressors: Flow Phenomena and Performance, Brussels, 7–9 May 1980*

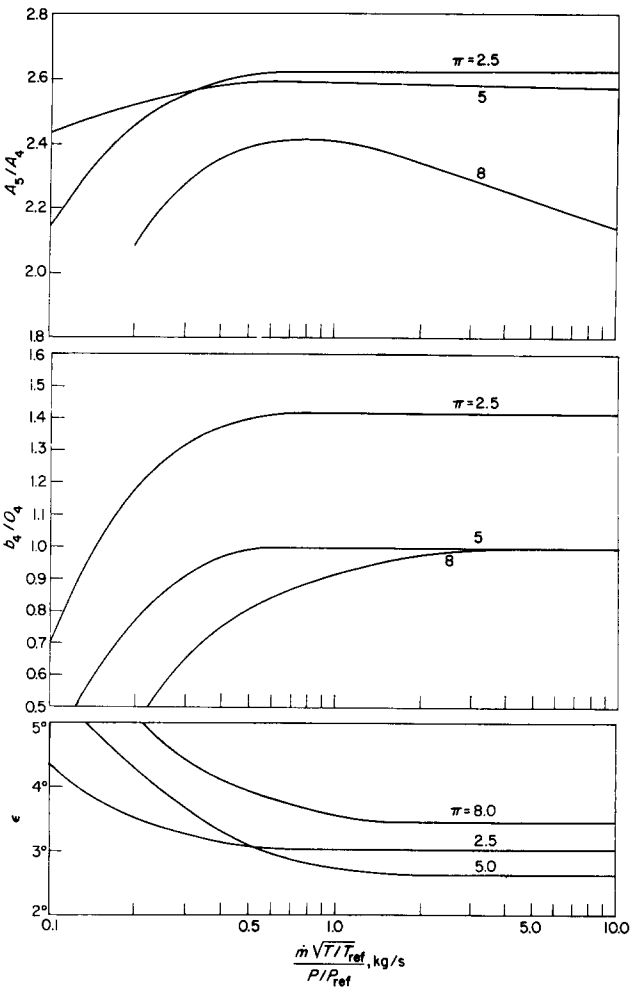

Fig 10 Geometric features of the diffuser (a) Area ratio A_5/A_4*; (b) Aspect ratio* b_4/O_4*; and (c) Divergence half-angle of the channel* ε

16 **Vavra M. H.** Basic elements for advanced design of radial flow compressors. *AGARD Lecture notes 39 Advanced Compressors, Von Karman Institute, Brussels, 1–4 June 1970*

17 **Bammert K., Rautemberg M. and Wittekindt W.** Matching of turbocomponents described by the example of impeller and diffuser in a centrifugal compressor. *J. Eng. for Power*, **102**, *July 1980*

18 **Mashimo T. et al.** On the performance prediction of a centrifugal compressor scaled up. *ASME paper 82-GT-112, 1982*

19 **Japikse D.** Design optimization and performance map prediction for centrifugal compressors and radial inflow turbines. *AGARD L.S.83, June 1976*

20 **Dean R. C.** The fluid dynamic design of advanced centrifugal compressors. *Lecture notes 50, Advanced Radial Compressors. Von Karman Institute, Brussels, May 1975*

21 **Jansen W.** Steady fluid flow in a radial vaneless diffuser. *ASME paper 63-WA-12, 1963*

22 **Japikse D.** Life evaluation of advanced turbomachinery. *LS. on turbine blade cooling, Von Karman Institute, Jan. 1976*

BOOK REVIEW

Fluidized Bed Combustion and Applied Technology

Ed. R. G. Schwieger

This book contains 36 papers presented at the First International Fluidized Bed Combustion (FBC) Symposium held in Beijing, People's Republic of China (PRC) in August 1983. It has about 600 pages and more than 400 tables, charts, diagrams and photographs are supplied on the topics covered. Most of the papers are from PRC and USA. However, samples of work accomplished in 9 countries (Belgium, Canada, Denmark, UK, France, West Germany, Japan, Netherlands and Sweden) by industry, government research institutions and universities are also included.

The book is divided into five sections: overview, theory, design and development, environmental considerations, and operating data. Important aspects of fluidized bed combustion are touched upon in these sections. Some of the topics included are: a review of the state-of-the-art, combustion phenomena, heat transfer, modelling, pollution control and erosion of tubes in the bed. Atmospheric and pressurised fluidized bed combustion are discussed. Operations with low quality fuels such as oil shale, process char, extremely poor grades of coal and regular coal are described.

One of the attractive features of the book is that it contains extensive information on the experience of PRC in the area of fluidized bed combustion. Fluidized bed combustors and boilers have been used in PRC for the last 20 years to produce industrial steam and electricity. These units are locally built and run by average factory workers after a short training period. The experimental data and information on this experience should be valuable to industries manufacturing small combustors burning coal or other solid fuels, as well as to industries who are considering installing fluidized bed combustors in their facilities. There are also large amounts of data obtained from small and large units operating in other countries participating in the symposium. Empirical relations important for design purposes are given.

The book is an important source of information and a good reference for industry using or manufacturing combustors, and for researchers working in this or related areas in universities and government research institutions.

S. Yavuzkurt
Department of Mechanical Engineering,
The Pennsylvania State University,
USA

Published, price $95.00, by Hemisphere Publishing Corporation, Berkeley Building, 19W 44th Street, NY 10036, USA

Books received

Computational Fluid Mechanics and Heat Transfer, *D. A. Anderson, J. C. Tannehill and R. H. Pletcher*, $39.95, pp 599, Hemisphere

Perturbation Methods in Heat Transfer, *A. Aziz and T. Y. Na*, $37.50, pp 199, Hemisphere/Springer-Verlag

Steam tables (in SI-units) Wasserdampftafeln, *eds U. Grigull, J. Straub and P. Schiebener*, pp 94, DM 26, Springer-Verlag

Contains tables and diagrams concerning the properties of water and steam for use by students and research and industrial engineers to solve problems in power and chemical engineering. Thermodynamic properties have been calculated according to the formulation by Haar, Gallagher and Kell, adopted in 1983 by the 'International Association for the Properties of Steam'.

Steam tables, *eds L. Haar, J. S. Gallagher and G. S. Kell*, $34.50 (cloth), $14.95 (paper), pp 320, Hemisphere

Heat Exchanger Design Handbook, supplement 1, *eds E. U. Schlunder, K. J. Bell, D. Chisholm, V. Gnielinski, G. F. Hewitt, E. A. D. Saunders, F. W. Schmidt, D. B. Spalding, J. Taborek and A. Zukauskas*, pp 134, $115.00, Hemisphere/Springer-Verlag

Supplement 1 adds new technical data to the core handbook and includes: rules, practices and conversion charts; regeneration and thermal energy storage; waste heat boiler systems; fouling in heat exchangers; and properties of liquid heavy water.

Inclusion of a title in this section does not necessarily preclude subsequent review.